

Bond mechanism effect on the flexural behavior of steel reinforced concrete composite members

Jia-Ling Juang[†] and Hsieh-Lung Hsu[‡]

Department of Civil Engineering, National Central University, Chung-Li 32054, Taiwan

(Received July 6, 2005, Accepted March 27, 2006)

Abstract. This paper discusses the composite mechanism and its effect upon the behavior of a steel reinforced concrete (SRC) member subjected to a flexural load. The relationship between member strength and deformation is established using the bond strength between the steel and reinforced concrete. An analytical model is proposed and used to incorporate the sectional strains and bond strength at the elastic and inelastic stages for moment-curvature relationship derivation. The results from the flexural load tests are used to validate the accuracy of the proposed model. Comparisons between the experimental information and the analytical results demonstrate close moment-curvature relevance, which justifies the applicability of the proposed method.

Keywords: bond mechanism; bond strength; flexural behavior; deformation; composite members.

1. Introduction

Steel reinforced concrete (SRC) members consisting of structural steel and reinforced concrete possess high load-carrying performance and are effective structural forms for building and bridge construction. Besides the high steel strength and effective stiffness due to reinforced concrete, an effective bond mechanism between the structural steel and reinforced concrete significantly contributes to the SRC performance (Ricles and Paboojian 1994, Weng *et al.* 2001, 2002). It has been observed in the author's previous experimental investigations (Hsu and Wang 2002) that the local buckling tendency of steel within SRC composite members is significantly reduced and the flexural strength of the composite member, because of the bond mechanism, is higher than the sum of the individual steel and reinforced concrete strength.

Current information on SRC composite member design focuses primarily on member strength calculations, e.g. the ACI-318 (2002) design equation for composite member strength. In this design guide, a fully composite mechanism and compatible steel-concrete strain distribution, as shown in Fig. 1, is assumed throughout the load-carrying path, both in the elastic and inelastic stages. This assumption raises concerns about whether the calculated member strength could be over-estimated or the achievable deformation associated with the calculated maximum strength biased because the bond conditions might degrade, particularly during the elastic-plastic range, when member deformation increases causing concrete cracks on the members. Fig. 1 describes the deformation condition of a partially

[†]Ph.D. Candidate

[‡]Professor, Corresponding author, E-mail: T3200178@ncu.edu.tw

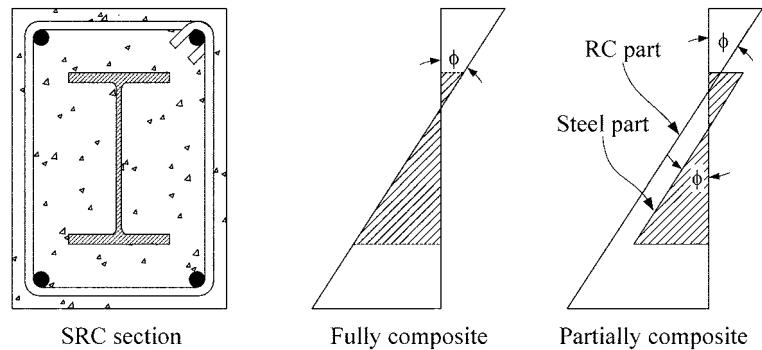


Fig. 1 Strain distribution of SRC section at various bond conditions

composite section. Accordingly, the evaluated structural responses and the subsequent implementation in engineering practices, based on the fully composite mechanism might be inadequate for effective structural designs. Therefore, analytical model investigation to rationally define the relationship between the bond mechanism and the member behavior, both in the elastic and inelastic stages, is necessary to provide adequate design information (Kwak and Kim 2001).

In general, the effectiveness between the structural steel and concrete composite mechanism in SRC members can be affected by many parameters. For example, the contact surface condition (Bryson and Mathey 1962), magnitude of member curvature, ϕ , as is defined in Fig. 1, and presence of cracks, etc. These factors produce a complicated and highly non-linear problem when the composite mechanism and member behavior are correlated. To make this investigation feasible, an experimental program, described below, was conducted first to establish the response references for the subsequent analytical study.

2. Experimental program

Six specimens, including three steel members with different cross sections: JIS H200×100×5.5×8, H194×150×6×9, H200×200×8×12; and three SRC members composed of steel sections identical to the previous steel members were fabricated for testing. These specimens were categorized as S-series and SRC-series, respectively, and used to investigate the relationship between the member behavior and the steel-concrete composite mechanism. The yield strength for the structural steel was 312 MPa. Longitudinal bars and stirrups for the reinforced concrete for the SRC sections were composed of four #6 deformed bars and #3 deformed bars at 100-mm spacing. The yield strengths for the #6 and #3 bars were 529.2 MPa and 563.2 MPa, respectively. The compressive strength of the concrete was 38.5 MPa. The specimen details are listed in Table 1 and shown in Fig. 2.

In each loading test, the specimen bottom was rigidly clamped by a pair of stiffened platform, and the member tip was attached to a servo-controlled hydraulic actuator for load transmission. Each specimen was subjected to an increasing flexural load by the prescribed increasing displacement, until the member reached the inelastic stage. The test setup is shown in Fig. 3(a). Strain gauges were mounted on the steel sections and the longitudinal bars of reinforced concrete to evaluate the strains, sectional curvatures and the corresponding member resistance at various load stages. Strain gauge arrangements are shown in Fig. 3(b). The load deformation relationship was established by integrating the stress

Table 1 Specimen labels and dimensions

Test group	Specimen No.	Steel section $d \times b_f \times t_w \times t_f$ (mm)	Rebar	Steel ratio ρ_s (%)
Steel	S100	H200×100×5.5×8	N.A.	N.A.
	S150	H194×150×6×9	N.A.	N.A.
	S200	H200×200×8×12	N.A.	N.A.
SRC	SRC100	H200×100×5.5×8	#6	1.9
	SRC150	H194×150×6×9	#6	2.8
	SRC200	H200×200×8×12	#6	4.6

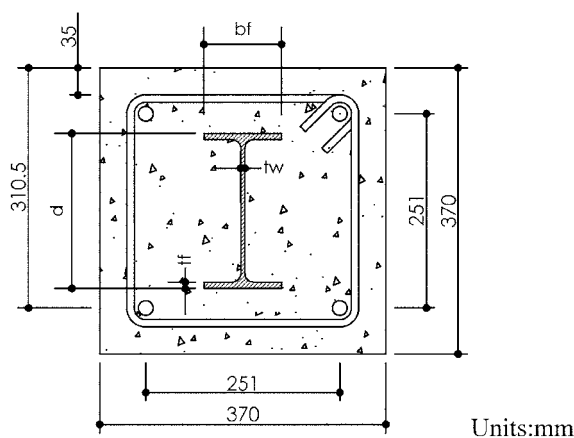


Fig. 2 Sectional details of the test specimens

blocks and the sectional curvatures, as discussed in subsequent sections, through the loading process.

As indicated in Fig. 1, a compatible strain distribution within the section must be maintained when the section is fully composite. In this case, identical curvature will be exhibited by the steel section and the reinforced concrete. However, when the member is subjected to larger deformation, the fully composite mechanism will begin to degrade and the strains on the steel section and reinforced concrete will deviate and redistribute, although the curvatures of these two parts will remain the same. Fig. 4 shows the curvatures of the tested members at various deformation magnitudes. The information presented in this figure complied with the above-mentioned phenomena.

In order to distinguish between the composite mechanism effect and the member behavior, the curvatures of the steel members and the steel section of the corresponding SRC members are further compared in Fig. 5. The figure shows that the steel curvature in the SRC members remained at the equivalent level of the steel member, both in the fully and partially composite stages. However, the SRC members' sectional neutral axes deviated causing parallel shifting in the steel strains. This phenomenon indicated that a particular bond mechanism, i.e., the longitudinal bond force resultant, caused axial strain in the SRC composite member. Variations in the magnitude of the bond strength at different composite states affect the sectional strain distribution, calculated strength, and accordingly, the member deformation. Therefore, an adequate analytical model investigation to take the bond mechanism into account and effectively define the load deformation relationship is essential.

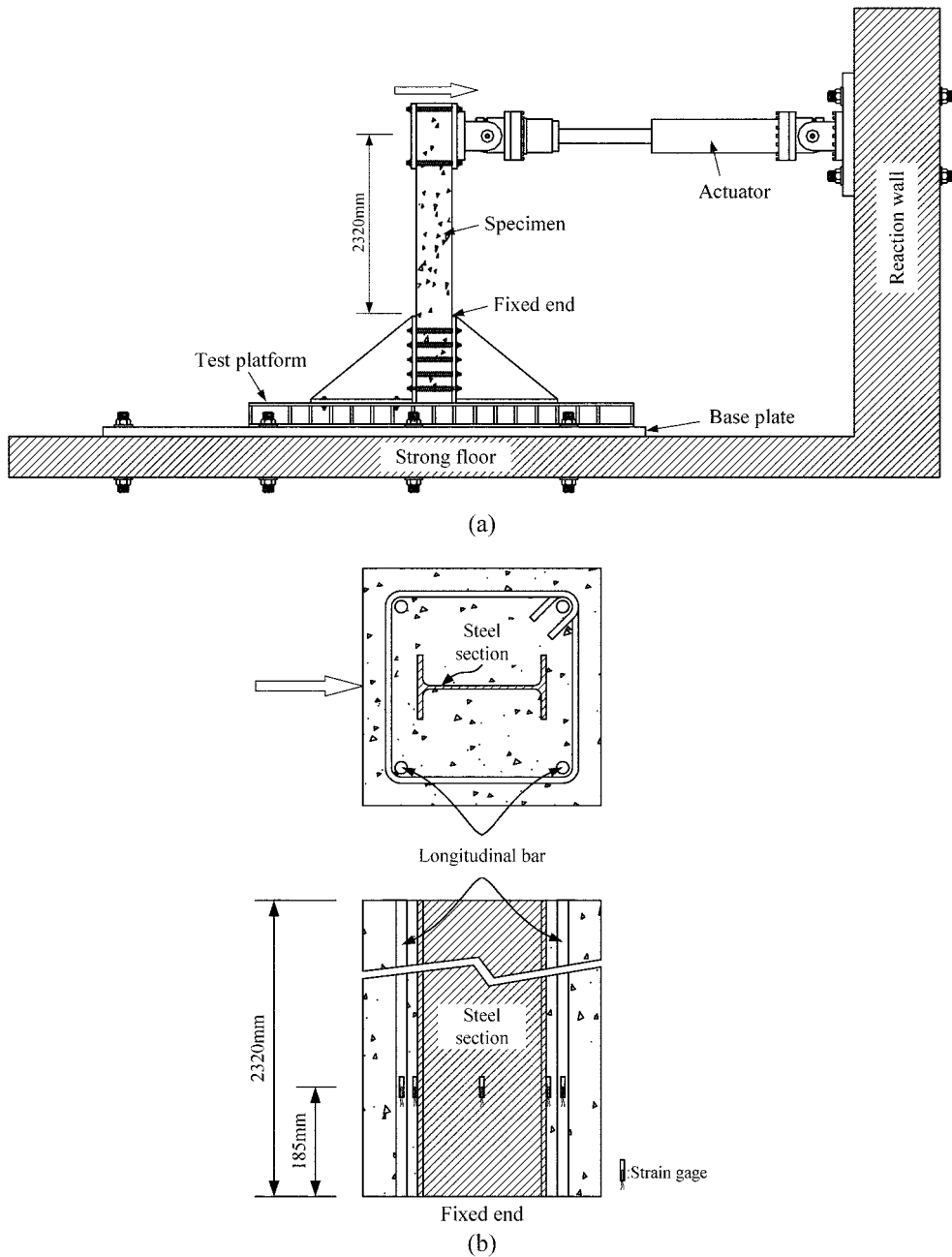


Fig. 3 Experimental program: (a) test setup, (b) strain gage arrangements

3. Analytical model

As mentioned above, the ACI-specified procedures for composite member strength calculations require full composite mechanism and compatible strain distribution between the steel and concrete

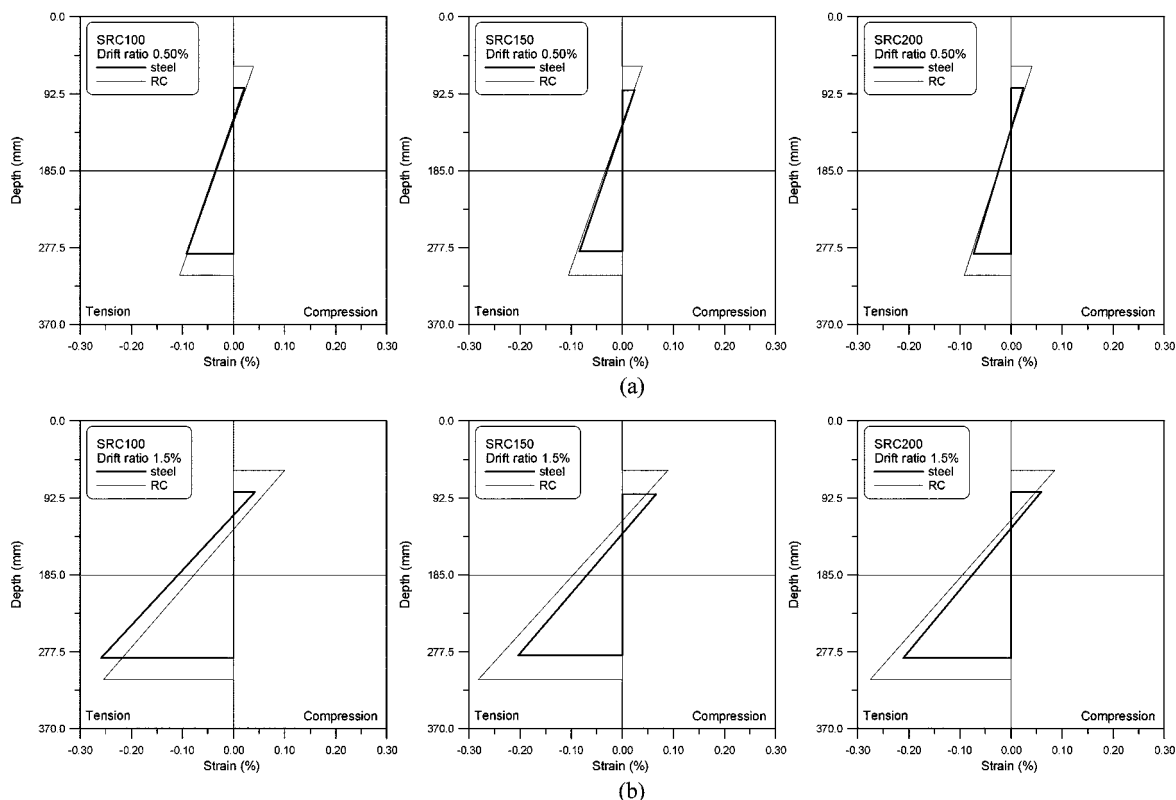


Fig. 4 Strain distributions of the steel and RC portions in the SRC section: (a) fully composite; (b) partially composite

throughout the load carrying process (Park and Paulay 1975, El-Tawil and Deierlein 1999, Yalcin and Saatcioglu 2000). This requires a highly iterative and cumbersome analytical process. To alleviate the calculation difficulty and acquire important load deformation information, not available in the current ACI process, a simple and effective approach that accounts for the bond strength between the steel and concrete at various load stages is adopted in this study.

3.1. Bond requirements

The strain distributions of the steel, reinforced concrete, and fully composite SRC sections are considered and shown in Fig. 6. The associated neutral axes of these sections, $(N.A.)_S$, $(N.A.)_{RC}$, and $(N.A.)_{SRC}$, will differ due to various sectional compositions. Because the neutral axis of the fully composite section deviates from its center of gravity, (C.G.), the magnitudes of the compressive and tensile strains on the steel section will be unequal. This is different from the strain responses of a steel-only section. Similarly, the compressive concrete strain on the fully composite section is also different from the strain value of the reinforced concrete section alone. The variations in strain distribution on the composite section and its components indicate that the bond strength between the steel and concrete effectively mobilizes steel and concrete deformation.

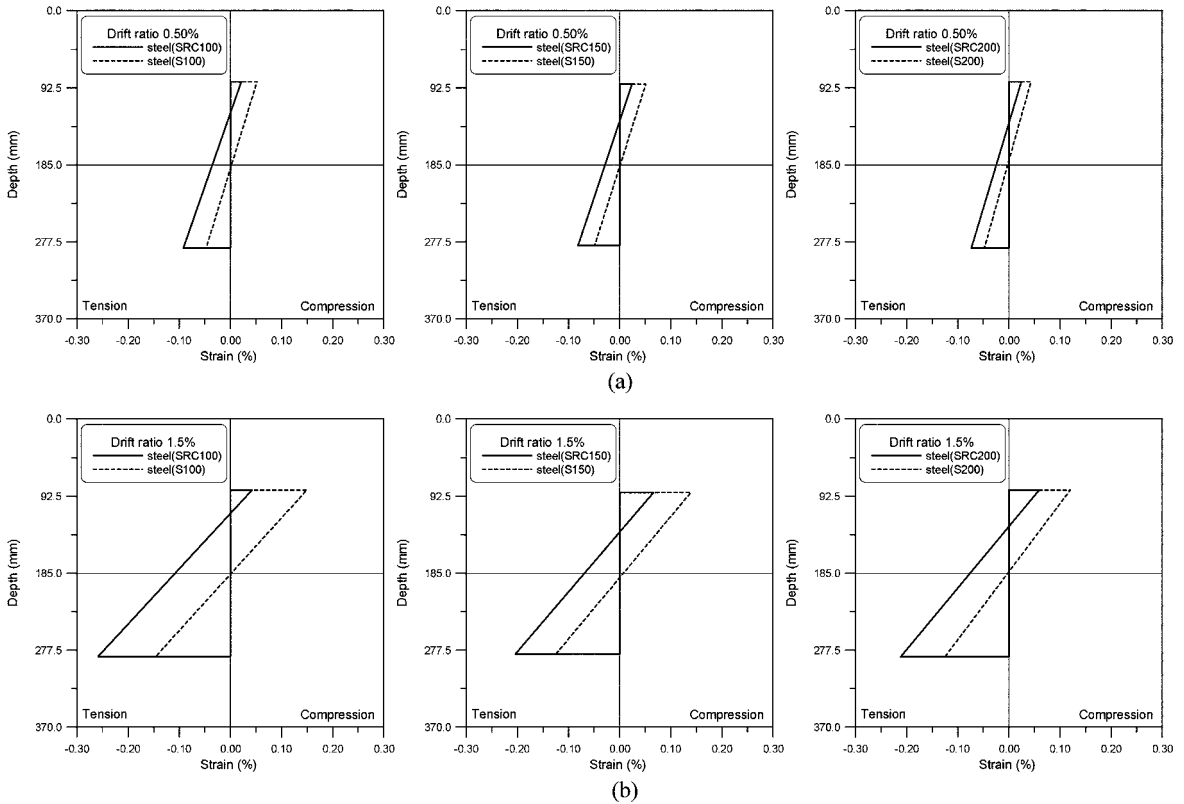


Fig. 5 Strain distributions of steel sections at various drift: (a) fully composite (drift=0.5%); (b) partially composite (drift=1.5%)

For a structural steel section subjected to bending, the compressive and the tensile forces induced on the section, C_{S0} and T_{S0} , as shown in Fig. 6(a), must be the same in magnitude and acting at the same distance measured from the center of gravity. That is:

$$C_{S0} = T_{S0} \tag{1}$$

Similarly, the resultant compressive and tensile forces induced on a reinforced concrete section due to external load, denoted C_{RC0} and T_{RC0} , will also be in equilibrium:

$$C_{RC0} = T_{RC0} \tag{2}$$

These equilibriums are altered when the structural steel is encased and fully bonded to the reinforced concrete forming a composite member. In this case, the sectional responses must be correlated using the following force equilibrium, as shown in Fig. 6(c), and expressed as:

$$C_{RC} + C_S = T_{RC} + T_S \tag{3}$$

in which C_{RC} and C_S are the resultant compressive forces acting on the composite section's reinforced

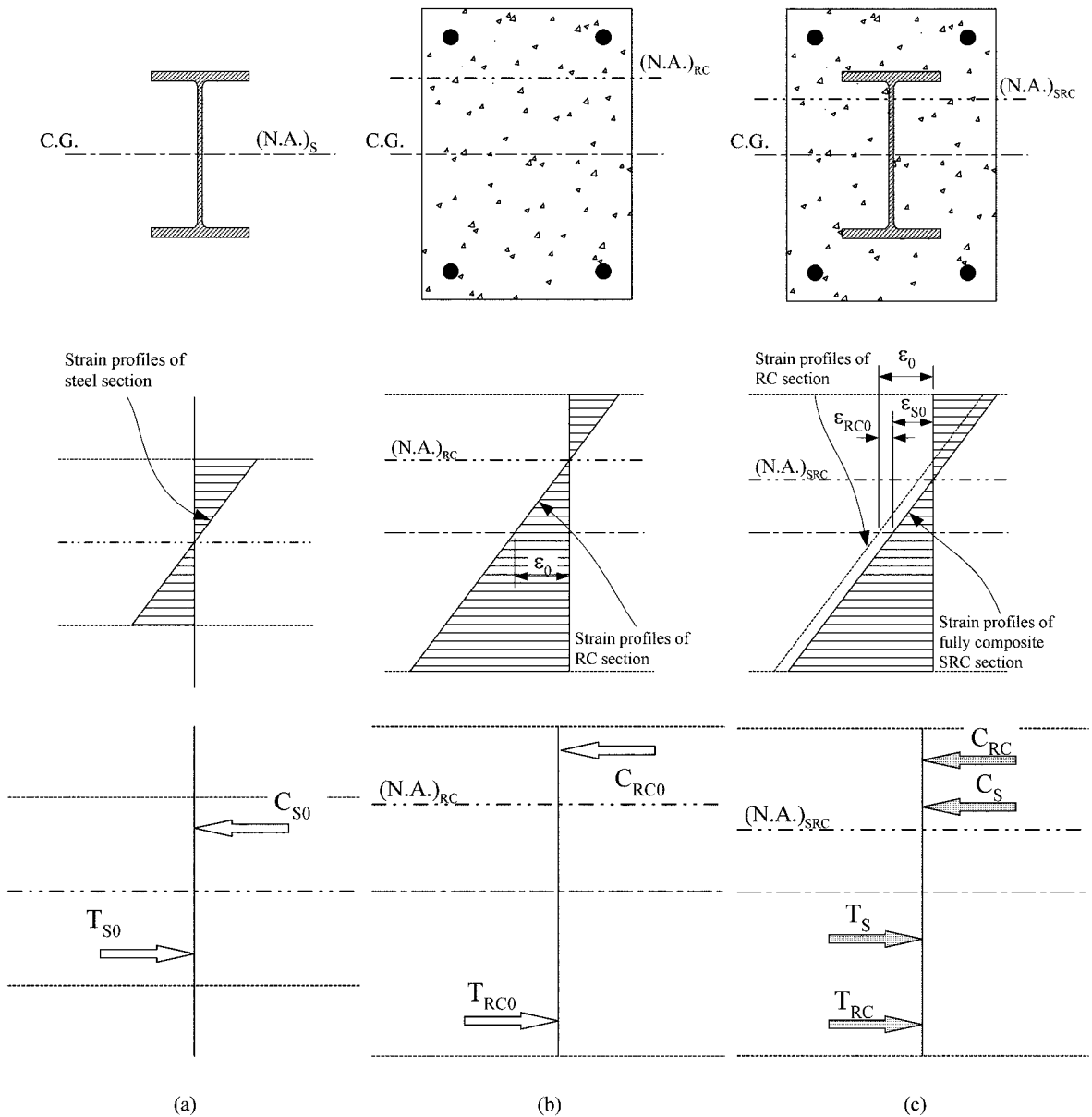


Fig. 6 Strain and internal force distributions for various sections: (a) steel only; (b) reinforced concrete; (c) SRC

concrete and steel portions; respectively. Similarly, T_{RC} and T_S are the tensile resultant forces acting on the composite section's reinforced concrete and steel portions. The parameters in Eq. (3) can be obtained by evaluating the strains, and subsequently, the stress blocks, as shown in Fig. 6(c). This can be found in the figure by comparing the strains at the center of gravity of the SRC sections where the bond strength induced increment and decrement of the tensile strains on the SRC section steel and concrete, denoted ϵ_{S0} and ϵ_{RC0} , respectively, than those on the individual steel-only or reinforced

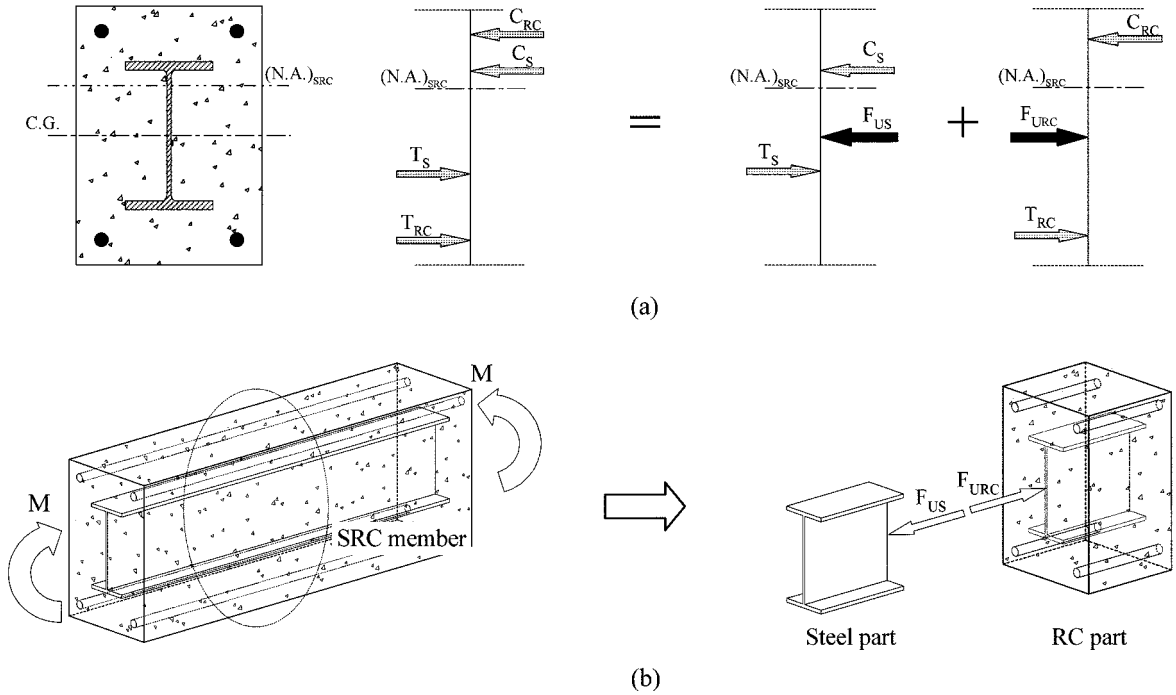


Fig. 7 Bond force distribution: (a) internal force; (b) three-dimensional sketch

concrete sections. To make the deformation compatible, the relationship between these values and the strain at the center of gravity of the reinforced concrete section, ϵ_0 , can be related and expressed as follows:

$$\epsilon_{S0} + \epsilon_{RC0} = \epsilon_0 \tag{4}$$

As shown in Fig. 7, the neutral axis of a composite section is located at a distance away from the section's center of gravity toward the section's compressive zone. Therefore, the resultant compressive force on the steel portion of the SRC section, C_S , is smaller than the tensile force, T_S . To balance the force acting on the SRC's steel section, an additive force, which is the bond force between the steel and reinforced concrete, must develop. This force is related to the bond stress exhibited on the contact surface between the steel and concrete. Because the structural steel is doubly-symmetric, the bond mechanism can be expressed using a resultant bond force, F_{US} , longitudinally acting on the steel center of gravity. Therefore, the following equilibrium can be established:

$$C_S + F_{US} = T_S \tag{5}$$

A similar phenomenon can be observed in the reinforced concrete portion of the SRC section. As shown in Fig. 6(b), the neutral axis of the composite section is shifted and becomes closer than the neutral axis of a reinforced concrete member toward the section's center of gravity. This means that a larger compressive area is achieved in the SRC section than that in a RC section only. The tensile force acting on the reinforced concrete portion of the SRC section, T_{RC} , is thus smaller than the compressive

force, C_{RC} . Therefore, an internal tensile force, F_{URC} , must be induced to achieve the equilibrium. This mechanism results in the following expression:

$$C_{RC} = T_{RC} + F_{URC} \quad (6)$$

Since the bond force between the steel and reinforced concrete is an internal force and must be in self-equilibrium, they can be equated and expressed using a single parameter F_{br} :

$$F_{US} = F_{URC} = F_{br} \quad (7)$$

This value indicates the bond requirement for a fully-composite section.

As indicated above, the tensile strain increment on the steel of a composite section is ε_{S0} . This value is due to inter-facial force application, F_{br} , and can be expressed as:

$$\varepsilon_{S0} = \frac{F_{br}}{E_S A_S} \quad (8)$$

in which E_S and A_S are the Young's modulus and cross-sectional area of the steel.

Similarly, the compressive strain increment on the reinforced concrete of the composite section, ε_{RC0} , can be expressed as:

$$\varepsilon_{RC0} = \frac{F_{br}}{(EA)_{RC}} \quad (9)$$

where, $(EA)_{RC}$ is the equivalent axial rigidity of the reinforced concrete, and can be evaluated using:

$$(EA)_{RC} = E_C A_{CC} + E_b A_b \quad (10)$$

In which E_C , E_b are the moduli of elasticity of the concrete and longitudinal bars, and A_{CC} and A_b are the concrete area under compression and the total cross-sectional area of the longitudinal bars, respectively.

The bond requirement, F_{br} , for the composite mechanism at various deformation stages thus can be established by equating Eqs. (8), (9), and (4), and expressed as follows:

$$F_{br} = \frac{(EA)_{RC} E_S A_S}{(EA)_{RC} + E_S A_S} \varepsilon_0 \quad (11)$$

3.2. Bond strength

In order to evaluate the bond effectiveness during the loading process, the bond strength between the steel and concrete, F_{bs} , must be compared with the bond requirement, F_{br} . According to the study by Roeder (1999), the bond strength per unit area, f_b (MPa), is a function of the ratio between the steel and composite section areas, ρ_S , and can be expressed as follows:

$$f_b = 1.256 - 9.554 \rho_S \quad (12)$$

This bond strength is assumed uniformly distributed around the steel contour to an effective length, L_{Ub} , when the members were subjected to an applied load. The value for L_{Ub} can be expressed as follows:

$$L_{Ub} = (3.22 - 24.519\rho_s)d \tag{13}$$

in which d is the depth of the structural steel. Therefore, the resultant bond strength between the steel and concrete, F_{bs} , can be evaluated using the following expression:

$$F_{bs} = f_b L_{Ub} L_{SS} \tag{14}$$

In which L_{SS} is the length of the contact surface between the steel and concrete. As long as the bond strength, F_{bs} , is greater than the bond requirement, F_{br} , a fully composite section is maintained.

3.3. Behavior at inelastic stage

As indicated in Eq. (11), the bond requirement increases when the sectional strain and the curvature increase. Because the bond strength is limited, a bond degradation state will develop when the bond requirement becomes higher due to a larger deformation that exceeds the bond strength. To adequately illustrate the relationship between member deformation and the corresponding load, a modified model that describes the bond mechanism and evaluates the member strength must be adopted. It has been demonstrated that residual bond strength after the initiation of bond degradation, f'_b , can be represented using a fraction of the original strength, shown in Fig. 8, as follows:

$$f'_b = f_b - \alpha^*(\varepsilon - \varepsilon_b) \tag{15}$$

In which α^* is a strain-dependant bond strength reduction factor, and ε_b is the strain associated with the initiation of bond strength degradation. The value ε_b can be determined using the following expression:

$$\varepsilon_b = \frac{F_{bs}}{A_s E_s} \tag{16}$$

Therefore, the bond strength at the inelastic stage, F'_{bs} , can be evaluated by replacing f_b in Eq. (14) with f'_b to obtain the following expression:

$$F'_{bs} = f'_b L_{Ub} L_{SS} \tag{17}$$

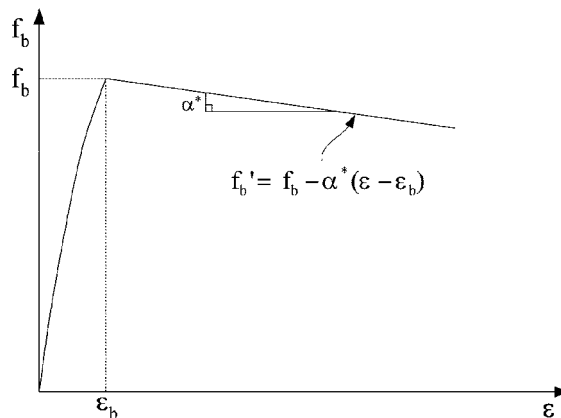


Fig. 8 Relationship between bond strength and sectional strain

4. Validation of proposed model

The member strength at the elastic and inelastic stages, M_e and M_{ie} , respectively, can be evaluated using the couple action from the resultant tensile and compressive force, as shown in Fig. 9, and expressed by the following:

Elastic stage

$$M_e = \Sigma C_{SRC} \cdot d_i \tag{18}$$

Inelastic stage

$$M_{ie} = \Sigma C'_{SRC} \cdot d'_i \tag{19}$$

in which ΣC_{SRC} and $\Sigma C'_{SRC}$ are the resultant compressive force at the elastic and inelastic stages, respectively, and d_i and d'_i are the distance between the resistance centers of the resultant compressive and tensile forces at the corresponding loading stages. Based on the theorem of equilibrium, the resultant compressive and tensile forces are equal and opposite in direction, both in elastic and inelastic stages, and can be evaluated by the following expressions:

Elastic stage

$$\Sigma C_{SRC} = \Sigma T_{SRC} = C_{RC} + C_S \tag{20}$$

Inelastic stage

$$\Sigma C'_{SRC} = \Sigma T'_{SRC} = C'_{RC} + C'_S \tag{21}$$

The difference between Eqs. (20) and (21) is that the values C_{RC} , C_S ; and C'_{RC} , C'_S are calculated with respect to the effective sections in the elastic and inelastic stages, respectively.

Fig. 10 shows the procedures for establishing the load deformation relationships. Table 2 lists the corresponding moment strengths at typical curvature points obtained from the tests and the analytical procedures. The comparisons between the experimental and analytical results in the moment-curvature relationships for the composite SRC members are also shown in Fig. 11. The figure shows that significant relevance was achieved, which justifies the applicability of the proposed method in SRC member behavior analyses.

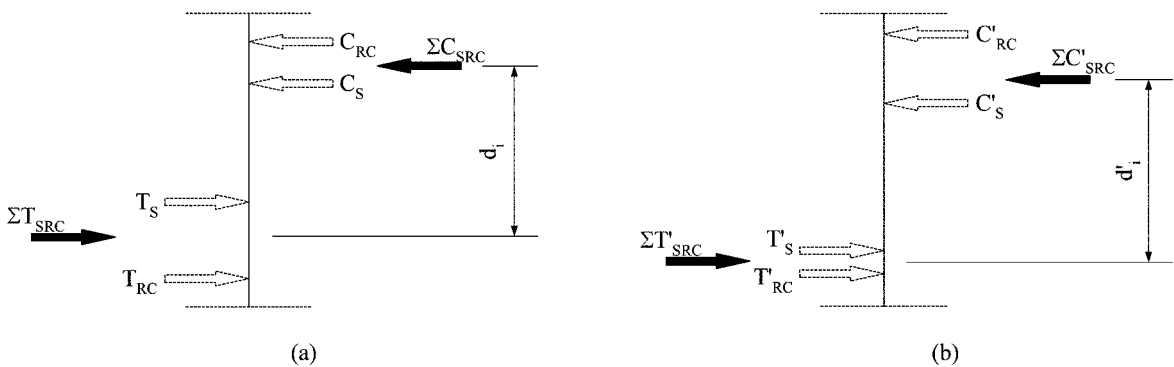


Fig. 9 Member strength calculations: (a) elastic stage; (b) inelastic stage

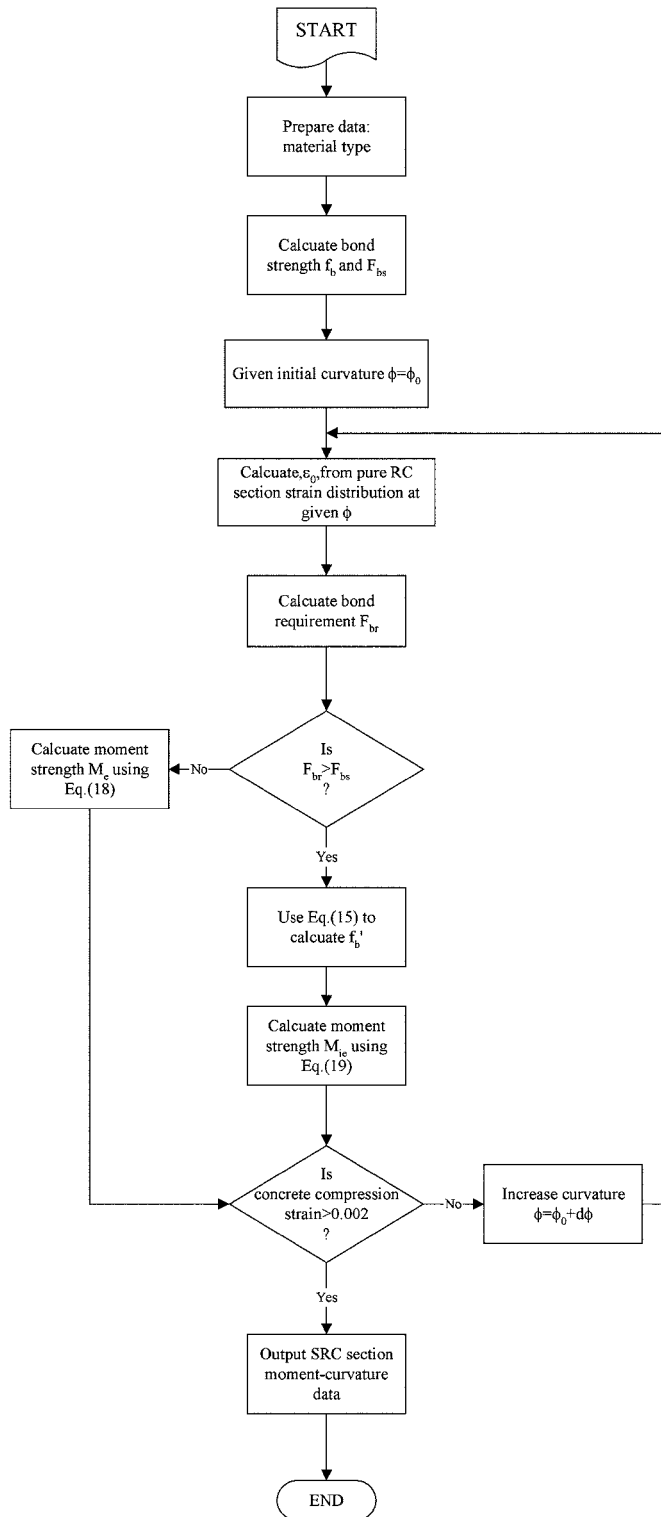


Fig. 10 Derivation procedures for SRC moment-curvature relationship

Table 2 Analytic moment strength compare with experimental result

Curvature (1/m)	Corresponding moment (kN-m)					
	SRC100		SRC150		SRC200	
	Analytic	Experimental	Analytic	Experimental	Analytic	Experimental
0.005	85.174	84.3724	91.279	92.315	129.636	131.208
0.010	156.526	153.752	172.872	179.714	217.610	220.232
0.015	168.460	160.181	209.894	207.037	270.960	273.051
0.020	171.413	166.369	215.801	214.631	279.135	280.166

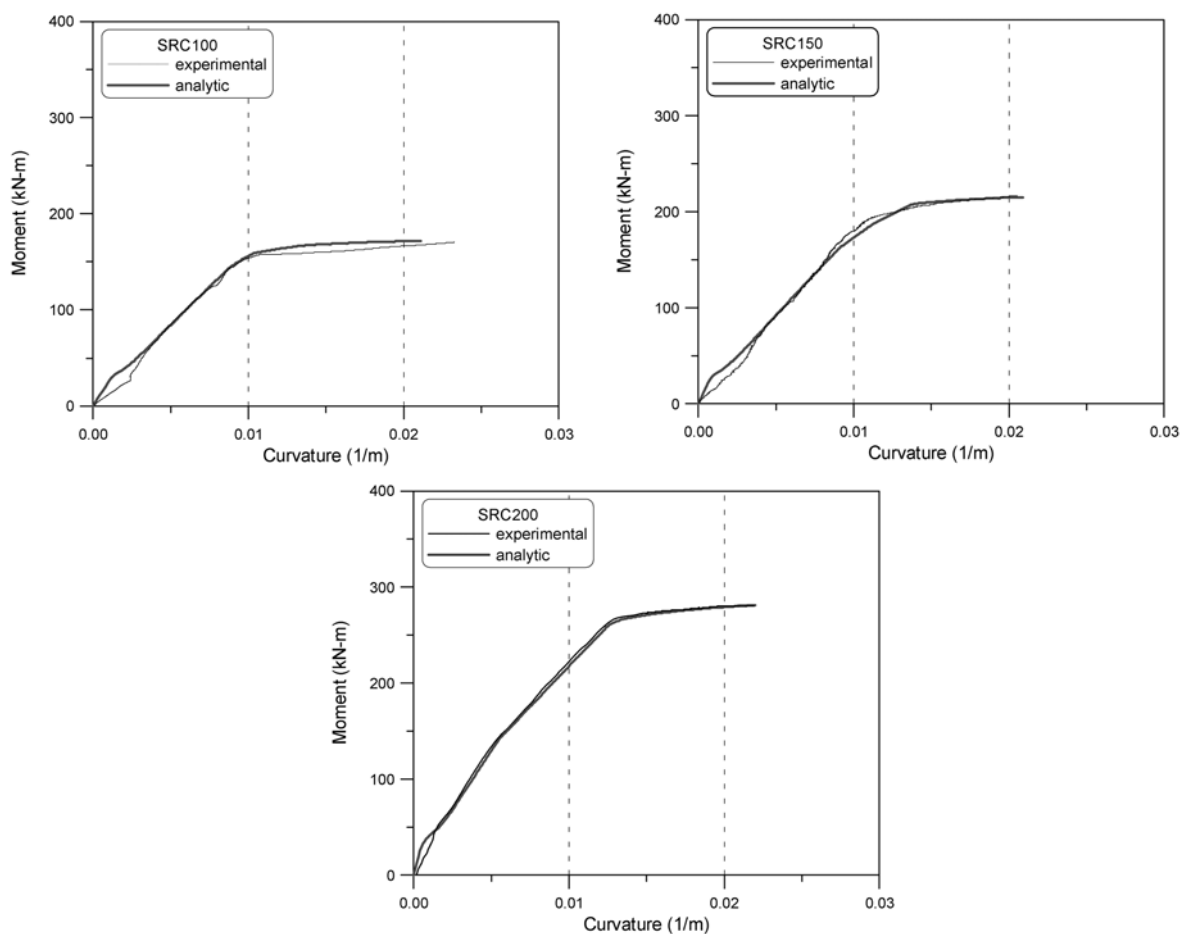


Fig. 11 Comparisons of analytical and experimental results

5. Conclusions

This study investigated the composite mechanism and its effect upon the behavior of an SRC member subjected to a flexural load. Specimens with various sectional compositions were fabricated and tested under flexural loads to obtain the member responses. The relationship between the member strength

and deformation was established by considering the bond mechanism between the steel and reinforced concrete. An analytical model that incorporated the sectional strains and the elastic and inelastic bond mechanism was proposed for moment-curvature relationship derivation. The results from the flexural load tests were used to validate the accuracy of the proposed model. Comparisons between the experimental information and the analytical results demonstrate that close relevance was achieved, which justifies the applicability of the proposed method.

Acknowledgements

This study was partially supported by the National Science Council of the Republic of China under Grant No. NSC92-2211-E-008-041, which is gratefully acknowledged.

References

- American Concrete Institute (ACI). (2002), *Buildings Code Requirements for Structural Concrete (ACI 318-02) and Commentary (ACI 318R-02)*. Farmington Hills, Michigan.
- Bryson, J. O. and Mathey, R. G. (1962), "Surface condition effect on bond strength of steel beams embedded in concrete", *J. Am. Concrete Inst.*, **59**(3), 397-405.
- El-Tawil, S. and Deierlein, G. G. (1999), "Strength and ductility of concrete encased composite columns", *J. Struct. Eng.*, **125**(9), 1009-1019.
- Hsu, H. L. and Wang, C. L. (2000), "Flexural-torsional behaviour of steel reinforced concrete members subjected to repeated loading", *Earthq. Eng. Struct. Dyn.*, **29**(5), 667-682.
- Kwak, H. G. and Kim, S. P. (2001), "Bond-slip behavior under monotonic uniaxial loads", *Eng. Struct.*, **23**(3), 298-309.
- Park, R. and Paulay, T. (1975), *Reinforced Concrete Structures*, Wiley, NY.
- Paulay, T. and Priestley, M. J. N. (1992), *Seismic Design of Reinforced Concrete and Masonry Buildings*, Wiley, NY.
- Ricles, J. M. and Paboojian, S. D. (1994), "Seismic performance of steel-encased composite columns", *J. Struct. Eng.*, **120**(8), 2474-2494.
- Roeder, C. W., Chmielowski, R. and Brown, C. B. (1999), "Shear connector requirements for embedded steel sections", *J. Struct. Eng.*, **125**(2), 142-151.
- Yalcin, C. and Saatcioglu, M. (2000) "Inelastic analysis of reinforced concrete columns", *Comput. Struct.*, **77**(6) 539-555.
- Weng, C. C., Yen, S. I. and Chen, C. C. (2001), "Shear-strength of concrete-encased composite structural members", *J. Struct. Eng.*, **127**(10), 1190-1197.
- Weng, C. C., Yen, S. I. and Jiang, M. H. (2002), "Experimental study on shear splitting failure of full-scale composite concrete encased steel beams", *J. Struct. Eng.*, **128**(9), 1186-1194.